

Nonstabilizerness via matrix product states in the Pauli basis

Poetri Sonya Tarabunga,^{1,2,3} Emanuele Tirrito,^{1,4} Mari Carmen Banuls,⁵ and Marcello Dalmonte^{1,2}

¹*The Abdus Salam International Centre for Theoretical Physics (ICTP), Strada Costiera 11, 34151 Trieste, Italy*

²*SISSA, Via Bonomea 265, 34136 Trieste, Italy*

³*INFN, Sezione di Trieste, Via Valerio 2, 34127 Trieste, Italy*

⁴*Pitaevskii BEC Center, CNR-INO and Dipartimento di Fisica, Università di Trento, Via Sommarive 14, Trento, I-38123, Italy*

⁵*Max-Planck-Institut für Quantenoptik, Hans-Kopfermann-Straße 1, D-85748 Garching, Germany and Munich Center for Quantum Science and Technology (MCQST), Schellingstraße 4, D-80799 Munich, Germany*

Nonstabilizerness, also known as “magic”, stands as a crucial resource for achieving a potential advantage in quantum computing. Its connection to many-body physical phenomena is poorly understood at present, mostly due to a lack of practical methods to compute it at large scales. We present a novel approach for the evaluation of nonstabilizerness within the framework of matrix product states (MPS), based on expressing the MPS directly in the Pauli basis. Our framework provides a powerful tool for efficiently calculating various measures of nonstabilizerness, including stabilizer Rényi entropies, stabilizer nullity, and Bell magic, and enables the learning of the stabilizer group of an MPS. We showcase the efficacy and versatility of our method in the ground states of Ising and XXZ spin chains, as well as in circuits dynamics that has recently been realized in Rydberg atom arrays, where we provide concrete benchmarks for future experiments on logical qubits up to twice the sizes already realized.

Introduction.— The simulation of quantum states is in general very hard for a classical computer [1]. For this reason, quantum physics could provide an advantage for this task [2]. It is well known that entanglement is a necessary resource to achieve this goal [3–10], but it is, however, not sufficient. In particular, there is a class of states called the stabilizer states that can be highly entangled, and yet it can be efficiently simulated classically [11–15]. As a result, universal quantum computation can only be achieved by utilizing non-Clifford resources. The amount of non-Clifford resources necessary to prepare a state is called nonstabilizerness, commonly referred to as “magic” [16–24], which is a fundamental resource to unlock potential quantum advantage.

Much like entanglement, nonstabilizerness has been quantified within the framework of resource theory using measures of nonstabilizerness [25]. Several measures of nonstabilizerness have been proposed in quantum information theory, with most of them relying on the notion of quasiprobability distributions [21, 23, 26–29]. However, most of these quantifiers are difficult to evaluate even numerically (see, e.g., Refs. [20, 30–35]). This computational intractability has hindered the task of quantifying nonstabilizerness beyond a few qubits, posing a major challenge in the field. To address this challenge, two computable and practical measures of nonstabilizerness have been introduced recently: the Bell magic [36] and the stabilizer Rényi entropies (SREs) [37]. Several methods have been put forward to compute the SREs, based on, e.g., tensor networks [38–41], Monte Carlo sampling of wavefunctions [42], and average over Clifford orbits [43, 44]. These methods have enabled the study of nonstabilizerness in many-body contexts, particularly its connection to criticality [39, 41, 42, 45, 46]. However, these approaches still face limitations in their applicabil-

ity and computational efficiency, especially in terms of demonstrated accessible quantities.

In this work, we demonstrate how, for quantum many-body states of MPS form, several nonstabilizerness measures can be cast in the language of tensor networks [47–52], whose contractions can be approximated using standard algorithms. More concretely, we represent the Pauli spectrum of the state as a matrix product state (MPS), cf. Fig. 1 (a,b), which represents the state in the Pauli basis. We show that such MPS representation can be used to compute not only the SRE, but also the Bell magic, which has so far not been quantified in large quantum systems, as it is too costly to compute by any of the existing methods. For the SRE in particular, we express it as a two-dimensional tensor network as shown in Fig. 1 (c), thereby providing a simple means to contract the tensor network using established MPS methods. Furthermore, we explain how to extract the stabilizer group of a state within our approach, which in turn allows us to compute the stabilizer nullity, a strong nonstabilizerness monotone. We benchmark our method through various examples, including the quantum Ising chain, the XXZ chain, and random Clifford circuits with nonstabilizer states input. We further applied our method to compute the Bell magic in a scrambling circuit (see Fig. 1 (d)) that has recently been experimentally implemented in Rydberg atom arrays [53]. Reaching system sizes beyond the current experimental capabilities, our method can thus be used to verify and benchmark future experiments.

MPS in the Pauli basis.— Let us consider a system of N qubits in a pure state $|\psi\rangle$ given by a MPS of bond

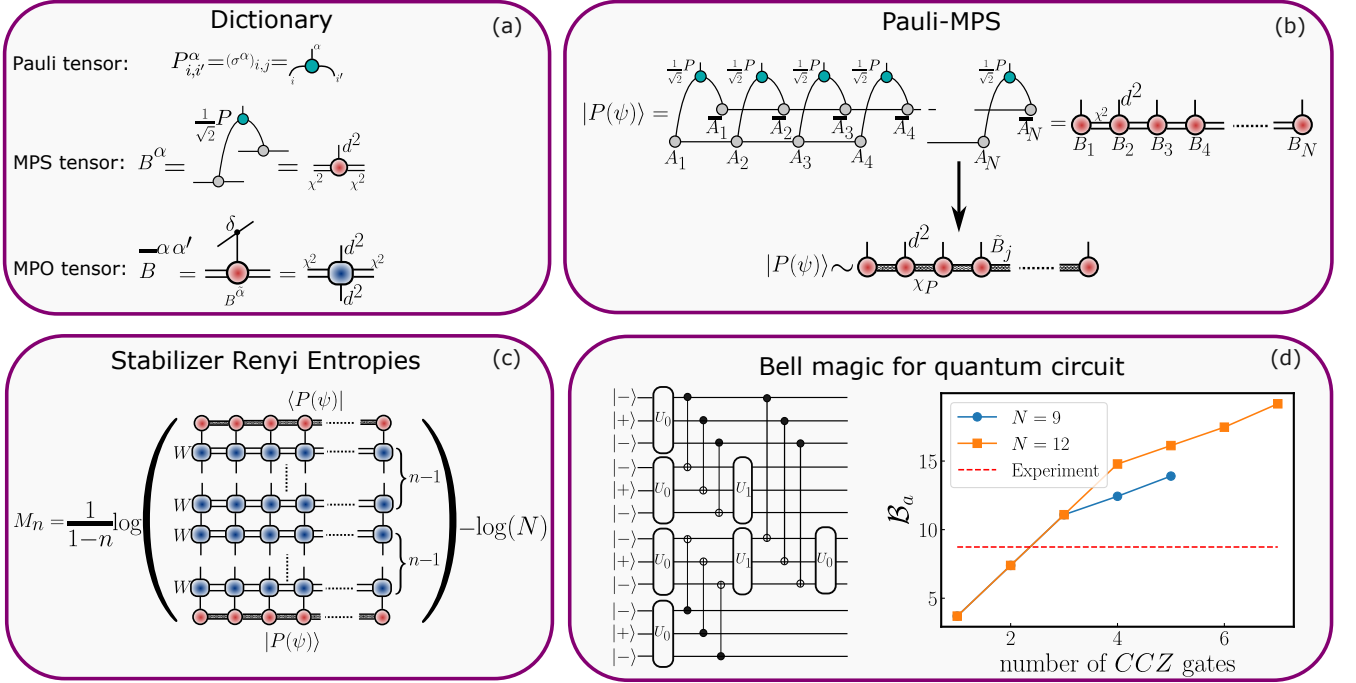


FIG. 1. (a) Definitions of tensors used for the construction of Pauli-MPS. (b) Construction of Pauli-MPS. (c) The SRE represented as the contraction of a two-dimensional tensor network. (d) The additive Bell magic in a scrambling circuit recently experimentally realized in Ref. [53]. The red dashed line indicates the highest value of the additive Bell magic experimentally measured in Ref. [53].

dimension χ :

$$|\psi\rangle = \sum_{s_1, s_2, \dots, s_N} A_1^{s_1} A_2^{s_2} \dots A_N^{s_N} |s_1, s_2, \dots, s_N\rangle \quad (1)$$

with $A_i^{s_i}$ being $\chi \times \chi$ matrices, except at the left (right) boundary where $A_1^{s_1}$ ($A_N^{s_N}$) is a $1 \times \chi$ ($\chi \times 1$) row (column) vector. Here $s_i \in \{0, 1\}$ is a local computational basis. The state is assumed right-normalised, namely $\sum_{s_i} A_i^{s_i \dagger} A_i^{s_i} = 1$. Let us define the binary string $\alpha = (\alpha_1, \dots, \alpha_N)$ with $\alpha_j \in \{00, 01, 10, 11\}$. The Pauli strings are defined as $P_{\alpha} = P_{\alpha_1} \otimes P_{\alpha_2} \otimes \dots \otimes P_{\alpha_N}$ where $P_{00} = I, P_{01} = \sigma^x, P_{11} = \sigma^y$, and $P_{10} = \sigma^z$. We define the Pauli vector of $|\psi\rangle$ as $|P(\psi)\rangle$ with elements $\langle \alpha | P(\psi) \rangle = \langle \psi | P_{\alpha} | \psi \rangle / \sqrt{2^N}$. Also known as the Pauli spectrum [54], this was recently studied in the context of many-body systems [55]. When $|\psi\rangle$ has an MPS structure as in Eq. (1), the Pauli vector can also be expressed as an MPS as follows

$$|P(\psi)\rangle = \sum_{\alpha_1, \alpha_2, \dots, \alpha_N} B_1^{\alpha_1} B_2^{\alpha_2} \dots B_N^{\alpha_N} |\alpha_1, \dots, \alpha_N\rangle \quad (2)$$

where $B_i^{\alpha_i} = \sum_{s, s'} \langle s | P_{\alpha_i} | s' \rangle A_i^s \otimes \overline{A_i^{s'}} / \sqrt{2}$ are $\chi^2 \times \chi^2$ matrices, as shown in Fig. 1. Note that the MPS is normalized due to the relation $\frac{1}{2^N} \sum_{\alpha} \langle \psi | P_{\alpha} | \psi \rangle^2 = 1$ which holds for pure states. Moreover, it retains the right normalization, due to the identity $\frac{1}{2} \sum_{\alpha} P_{\alpha}(\cdot) P_{\alpha} = \mathbb{1} \text{Tr}[\cdot]$.

Consequently, the entanglement spectrum of $|P(\psi)\rangle$ is given by $\lambda'_{i,j} = \lambda_i \lambda_j$ for $i, j = 1, 2, \dots, \chi$, where λ_i is the entanglement spectrum of $|\psi\rangle$, and hence the von Neumann entropy is doubled. Note also that the coefficients of $|P(\psi)\rangle$ in the Pauli basis (2) are real, since the Pauli operators are Hermitian for spin-1/2 systems, although the local tensors B_i are not necessarily real.

Since the Pauli operators provide an orthonormal basis in the space of Hermitian operators, one can expand the density matrix as $|\psi\rangle\langle\psi| = \frac{1}{2^N} \sum_{\alpha} \langle \psi | P_{\alpha} | \psi \rangle P_{\alpha}$. Therefore, the Pauli spectrum is simply the coefficients of $|\psi\rangle\langle\psi|$ in the basis of Pauli operators, i.e., the Pauli basis. However, constructing the MPS representation of the Pauli vector $|P(\psi)\rangle$ may appear to be unnecessarily costly, as the bond dimension is squared from that of the original MPS $|\psi\rangle$. As we show below, such MPS representation in the Pauli basis nevertheless provides a powerful and versatile tool to compute various measures of non-stabilizerness in the state $|\psi\rangle$. This is because the MPS representation provides direct access to the Pauli spectrum, in terms of which these nonstabilizerness measures are defined. Specifically, in the following we will consider the measures SRE [37], the stabilizer nullity [54], and the Bell magic [36].

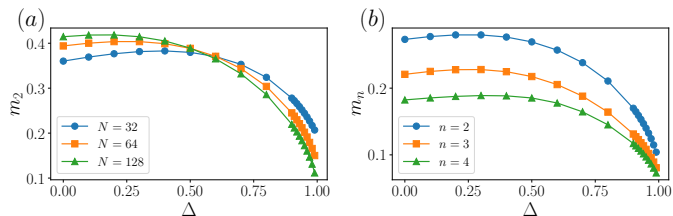


FIG. 2. SRE density $m_n = M_n/N$ for the ground state of the XXZ chain as a function of the anisotropy Δ for (a) $n = 2$ in various system sizes and (b) for $n \in \{2, 3, 4\}$ with $N = 64$.

The SRE is defined as [37]

$$M_n(|\psi\rangle) = \frac{1}{1-n} \log_2 \left\{ \sum_{\alpha} \frac{|\langle \psi | P_{\alpha} | \psi \rangle|^{2n}}{2^N} \right\}. \quad (3)$$

Then, the additive Bell magic $\mathcal{B}_a(|\psi\rangle)$ is given by

$$\mathcal{B}_a(|\psi\rangle) = -\log_2(1 - \mathcal{B}(|\psi\rangle)), \quad (4)$$

where $\mathcal{B}(|\psi\rangle)$ is the Bell magic, defined as [36]

$$\mathcal{B}(|\psi\rangle) = \sum_{\substack{\alpha, \alpha' \\ \beta, \beta'}} \Xi(\alpha)\Xi(\alpha')\Xi(\beta)\Xi(\beta') \|[P_{\alpha \oplus \alpha'}, P_{\beta \oplus \beta'}]\|_{\infty}, \quad (5)$$

where $\Xi(\alpha) = |\langle \psi | P_{\alpha} | \psi \rangle|^2 / 2^N$ is a probability distribution defined over the set of Pauli strings [56], also known as the characteristic function [57], and \oplus denotes a bit-wise XOR. The infinity norm is zero when the Pauli strings commute and 2 otherwise. Finally, the stabilizer nullity $\nu(|\psi\rangle)$ is simply related to the size of the stabilizer group $\text{Stab}(\psi)$, which is the group of Pauli strings that stabilize $|\psi\rangle$. The stabilizer nullity is defined as [54]

$$\nu(|\psi\rangle) = N - \log_2(|\text{Stab}(\psi)|). \quad (6)$$

More details on these measures can be found in [58]. Hereafter, we will drop the dependence on $|\psi\rangle$ to keep the notation light.

Replica MPS.— The replica method in MPS was introduced to compute the SRE of MPS in Ref. [39]. While exact, for practical purposes, the original formulation performed inferiorly with respect to Pauli sampling methods due to the extremely high cost with respect to the bond dimension [38, 40, 41]. Indeed, evaluating the SRE for an integer index $n > 1$ required a computational cost of $O(\chi^{6n})$, rendering it impractical for even the simplest case $n = 2$, where previous computations were restricted to $\chi = 12$ [38, 39]. Here, we show that the MPS in the Pauli basis can be exploited to significantly reduce the cost of the replica trick, making it superior also compared to sampling methods in terms of computational efficiency and flexibility.

To do so, we define a diagonal operator W whose diagonal elements are the components of the Pauli vector, $\langle \alpha' | W | \alpha \rangle = \delta_{\alpha', \alpha} \langle \alpha' | P(\psi) \rangle$. The MPO form of W reads

$$W = \sum_{\alpha, \alpha'} \bar{B}_1^{\alpha_1, \alpha'_1} \bar{B}_2^{\alpha_2, \alpha'_2} \dots \bar{B}_N^{\alpha_N, \alpha'_N} |\alpha_1, \dots, \alpha_N\rangle \langle \alpha'_1, \dots, \alpha'_N| \quad (7)$$

where $\bar{B}_i^{\alpha_i, \alpha'_i} = B_i^{\alpha_i} \delta_{\alpha_i, \alpha'_i}$. Applying $n - 1$ times W to $|P(\psi)\rangle$, we obtain $|P^{(n)}(\psi)\rangle = W^{n-1}|P(\psi)\rangle$, which is a vector with elements $\langle \alpha | P^{(n)}(\psi) \rangle = \langle \psi | P_{\alpha} | \psi \rangle^n / \sqrt{2^{Nn}}$. We denote the local tensors of $|P^{(n)}(\psi)\rangle$ by $B_i^{(n)\alpha_i}$. We have

$$\frac{1}{2^{Nn}} \sum_{\alpha} \langle \psi | P_{\alpha} | \psi \rangle^{2n} = \langle P^{(n)}(\psi) | P^{(n)}(\psi) \rangle \quad (8)$$

and [59]

$$M_n = \frac{1}{1-n} \log \langle P^{(n)}(\psi) | P^{(n)}(\psi) \rangle - \log N. \quad (9)$$

The exact bond dimension of $|P^{(n)}\rangle$ is $\min(\chi^{2n}, 4^{N/2})$, i.e., for large system sizes it grows exponentially with the order n , as the cost observed in Ref. [39]. However, by interpreting it as the repeated application of a MPO W onto an MPS, we can sequentially compress the resulting MPS after every iteration, and keep the best description of the resulting state as a MPS with some upper-bounded bond dimension χ_n [58]. This can be done with standard TNS routines used, e.g., in the simulation of time evolution [48, 60]. These methods allow us to monitor the error of the truncation, for example, by doing convergence analysis. [61]

The Pauli-MPS itself can also be approximated with a bond dimension $\chi_P < \chi^2$. The computational cost of this compression is $O(\chi_P^2 \chi^2 + \chi^3 \chi_P)$. Assuming $\chi_P \approx \chi$, this results in the overall cost of $O(\chi^4)$. By comparison, the computational cost of direct Pauli sampling is $O(N_S \chi^3)$ [38, 40], where N_S is the number of samples. Consequently, our method becomes superior compared to the latter when $N_S \gtrsim \chi$. Since N_S typically grows exponentially with N for the estimation of M_2 , our method vastly outperforms the sampling methods in terms of efficiency for large N . Although this is at the cost of computing an approximation to the quantity, the convergence can be analyzed with the standard TNS methods.

We illustrate the method by computing the SRE in the XXZ chain, $H_{\text{XXZ}} = -\sum_{(i,j)} [\sigma_i^x \sigma_j^x + \sigma_i^y \sigma_j^y + \Delta \sigma_i^z \sigma_j^z]$, previously considered in Ref. [38]. We first obtain the ground state using DMRG with $\chi = 60$ and compress the bond dimension of the Pauli vector to $\chi_P = 400$. Fig. 2 (a) shows the results for $n = 2$ in various system sizes up to $N = 128$. We note that the Rényi-2 SRE could not be computed accurately for $N > 30$ in the previous study [38]. The discussion about convergence with bond dimension within our approach can be found

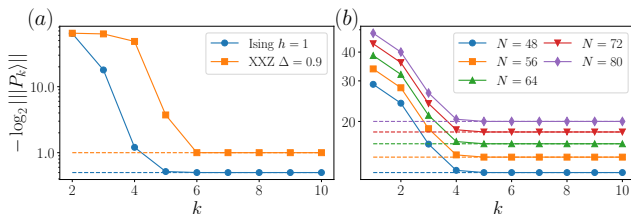


FIG. 3. We show $-\log_2 \| |P_k\rangle \|$ at iteration k in (a) the ground state of the quantum Ising chain at the critical point $h = 1$ and the XXZ chain at $\Delta = 0.9$ with $N = 128$, and (b) random quantum circuits with depth $D = N/4$ and $N_T = N/2$ number of T gates. After sufficiently many iterations, $-\log_2 \| |P_k\rangle \|$ flows to $(N - \nu)/2$. The dashed line denotes the analytically known $(N - \nu)/2$ for each system with the same color.

in [58]. Moreover, our method enables easier access to higher index SRE, as shown in Fig. 2 (b) for $n \in \{2, 3, 4\}$.

We further notice that the norm of $|P^{(n)}(\psi)\rangle$ can be interpreted as the contraction of a two-dimensional tensor network (see Fig. 1 (c)). This allows for alternative strategies to perform the contraction as for example transverse contractions [62–64], corner transfer matrix [65] or TRG techniques [66]. We leave these possibilities for future investigations (see [58]).

Bell magic.— Next, we consider Bell magic, a measure of nonstabilizerness [39] that has recently been experimentally measured in Ref. [53]. To compute the Bell magic, we first evaluate the self-convolution of $|P^{(2)}(\psi)\rangle$:

$$|Q(\psi)\rangle = \sum_{\alpha_1, \alpha_2, \dots, \alpha_N} C_1^{\alpha_1} C_2^{\alpha_2} \dots C_N^{\alpha_N} |\alpha_1, \dots, \alpha_N\rangle \quad (10)$$

where $C_i^{\alpha_i} = \sum_{\beta, \gamma} \delta_{\beta \oplus \gamma, \alpha_i} B_i^{(2)\beta} \otimes B_i^{(2)\gamma}$. Then, the additive Bell magic is given by

$$\mathcal{B}_\alpha = -\log \langle Q(\psi) | \Lambda \otimes \Lambda \otimes \dots \otimes \Lambda | Q(\psi) \rangle \quad (11)$$

where $\langle \alpha' | \Lambda | \alpha \rangle = 1$ if $[P_\alpha, P_{\alpha'}] = 0$ and $\langle \alpha' | \Lambda | \alpha \rangle = -1$ otherwise. The MPS $|Q(\psi)\rangle$, which has physical dimension 4 and exact bond dimension χ^8 , stores the probability distribution that can be obtained by Bell difference sampling [57]. As before, we can compress it to an MPS with smaller bond dimension to keep the computational cost manageable.

We have benchmarked the additive Bell magic calculations in the Ising and XXZ chains, where we find similar behavior to that of the SRE in both cases (see [58]). Furthermore, we computed the Bell magic in a state prepared by a quantum circuit recently realized in Ref. [53], shown in Fig. 1 (d). We verify that the additive Bell magic increases as a function of the number of CCZ gates applied. Similar growth of Bell magic can also be observed in T -doped random Clifford circuits [58].

Stabilizer nullity and stabilizer group.— Here, we show that the stabilizer nullity [54] can be calculated using MPS in the Pauli basis. The key insight is that the

stabilizer nullity can be expressed as a particular limit of the SRE:

$$\nu = \lim_{n \rightarrow \infty} (n - 1) M_n. \quad (12)$$

This is evident from Eq. (3), where taking the limit $n \rightarrow \infty$ effectively eliminates all Pauli strings except those for which $\langle \psi | P_\alpha | \psi \rangle = \pm 1$, i.e., those within the stabilizer group $\text{Stab}(\psi)$. We stress however that, unlike the SRE, the stabilizer nullity satisfies strong monotonicity [67].

Algorithm 1 Stabilizer nullity via Pauli-MPS

Input: Pauli vector $|P(\psi)\rangle$ and convergence tolerance ϵ

Output: Stabilizer nullity ν

```

1:  $|P_0\rangle \leftarrow |P(\psi)\rangle$ 
2:  $N_0 \leftarrow \| |P_0\rangle \|$ 
3:  $k \leftarrow 1$ 
4: repeat
5:    $|P_{k-1}\rangle \leftarrow |P_{k-1}\rangle / T_{k-1}$ 
6:    $W_k \leftarrow \text{diag}(|P_{k-1}\rangle)$ 
7:    $|P_k\rangle \leftarrow W_k |P_{k-1}\rangle$ 
8:    $T_k \leftarrow \| |P_k\rangle \|$ 
9:    $k \leftarrow k + 1$ 
10: until  $|1 - T_k / T_{k-1}| \leq \epsilon$ 
11:  $\nu \leftarrow N + 2 \log_2 T_k$ 

```

From Eq. (12) and Eq. (9), we see that the nullity can be obtained by applying W multiple times to $|P(\psi)\rangle$, normalizing the resulting MPS each time. This algorithm can be modified to reach the large n limit exponentially faster, following the trick employed in the exponential tensor renormalization group [68]. The idea is to construct a new MPO W_k after each iteration, which is a diagonal operator constructed out of the MPS $|P_k\rangle$ in the current iteration. The scheme is summarized in the Algorithm 1. After a number of iterations, the MPS will reach a fixed point $|G(\psi)\rangle$ which satisfies $W_\infty |G(\psi)\rangle = \sqrt{2^{\nu-N}} |G(\psi)\rangle$. One can see $|G(\psi)\rangle$ as the Pauli vector of $\rho^{(\infty)}$, whose Pauli expectation values are 1 if $\langle \psi | P_\alpha | \psi \rangle = \pm 1$, and 0 otherwise. $\rho^{(\infty)}$ is thus a (normalized) projector onto the stabilizer group of $|\psi\rangle$. The information about the stabilizer group of $|\psi\rangle$ can be extracted from $|G(\psi)\rangle$, since we have

$$\langle \alpha | G(\psi) \rangle = \begin{cases} \sqrt{2^{\nu-N}}, & \text{if } P_\alpha |\psi\rangle = \pm |\psi\rangle \\ 0, & \text{otherwise.} \end{cases} \quad (13)$$

The unsigned generators of the stabilizer group can be extracted using perfect MPS sampling [69] on $|G(\psi)\rangle$, which is efficient regardless of the size of the stabilizer group. Indeed, the protocol is equivalent to learning a stabilizer state by Bell sampling [70], which is always efficient as it only requires $O(N)$ samples. Once all the unsigned generators are found, the signs of the generators can be extracted from $|P(\psi)\rangle$. In this way, we are able to fully characterize the stabilizer group of $|\psi\rangle$ in a very efficient manner.

The learning of the stabilizer group has previously been used as a first step to learn the full description of T -doped stabilizer states [71–73]. Once the stabilizer group is obtained, one can efficiently construct a Clifford circuit C such that $C|\psi\rangle = |\phi\rangle \otimes |x\rangle$, where $|\phi\rangle$ is a state of ν qubits and $|x\rangle$ is a computational basis state of $N - \nu$ qubits. The learning of the state $|\psi\rangle$ is thus reduced to the learning of $|\phi\rangle$. Note that, while the MPS form itself is already an efficient classical description of a state, the description in terms of the stabilizer group could be of interest on its own, as it would be useful, e.g., in the context of Clifford circuits simulation. Furthermore, with the knowledge of the stabilizer group, one can construct a symmetric MPS in the Pauli basis, where the symmetry generators correspond to the generators of the stabilizer group. This approach could potentially reduce the computational complexity of MPS simulations in the Pauli basis.

To benchmark our algorithm, we consider the ground states of the Ising and XXZ chains. For the Ising chain, the nullity is $\nu = N - 1$ with stabilizer group $\{I_N, \prod_j \sigma_j^z\}$. For the XXZ chain, the nullity is $\nu = N - 2$ with stabilizer group $\{I_N, \prod_j \sigma_j^x, \prod_j \sigma_j^y, \prod_j \sigma_j^z\}$. The results of our algorithm are shown in Fig. 3 (a) for $N = 128$. We plot $-\log_2 \| |P_k\rangle \|$, which according to the algorithm above should flow to $\frac{N-\nu}{2}$ in the limit $k \rightarrow \infty$. We find that $-\log_2 \| |P_k\rangle \|$ reaches its expected value very quickly (in less than 10 iterations) in both cases.

Next, we consider a setup where a product state $|++++\dots\rangle$, for $|+\rangle = \frac{|0\rangle+|1\rangle}{\sqrt{2}}$, in a linear chain is doped with N_T number of T gates, where $T = e^{i\frac{\pi}{8}\sigma^z}$. We then apply a random Clifford circuit of depth D . The Clifford gates are drawn randomly from the set $\{S, H, CNOT, CZ\}$ in each layer. The two-qubit gates are applied only to nearest-neighbors. Notice that, applying our algorithm to a product state, the MPS $|P_k\rangle$ for each k is again a product state, and therefore the nullity can be computed very efficiently. As the stabilizer nullity is preserved by Clifford unitaries, the nullity of the final state is identical to the initial state, which is $\nu = N_T$. The application of Clifford gates will however increase the bond dimension of the MPS, such that the computation of the nullity becomes more difficult. We show the results for $D = N/4$ and $N_T = N/2$ in Fig. 3 (b) for system sizes $N = 48$ to $N = 80$. For this calculation, we allow the bond dimension to grow as needed to maintain a fixed truncation error threshold $\epsilon = 10^{-6}$. For $N = 80$, the bond dimension of the MPS reaches $\chi = 32$, while χ_P reaches $\chi_P = 1024$. We see again that $-\log_2 \| |P_k\rangle \|$ reaches its expected value in all cases.

Conclusions. — We have proposed a new MPS framework in the Pauli basis in order to investigate nonstabilizerness in quantum many-body systems. We discuss how several measures of nonstabilizerness, including the stabilizer Rényi entropies, the stabilizer nullity, and the

Bell magic can be efficiently approximated within our approach, and we demonstrated its usefulness in several scenarios, from ground states of spin chains to quantum circuits. Our framework can be easily generalized to mixed states and qudit systems, and it can be used to calculate nonstabilizerness in different partitions and in the context of perfect sampling [58].

In terms of future investigations, it would be interesting if our MPS approach could facilitate analytical treatment of the SRE in some exactly solvable models, by exploiting our simple interpretation of the SRE as a two-dimensional tensor network. Furthermore, we expect that our method would be useful to understand the role of nonstabilizerness in the context of hybrid quantum circuits, which has been the subject of recent works [74, 75]. In particular, our method allows for the efficient computation of the stabilizer nullity, which is a strong monotone, and is thus suitable to characterize nonstabilizerness in such scenarios. Finally, it would be fascinating to investigate whether our approach could be utilized to compute other nonstabilizerness measures that require optimization, such as the stabilizer fidelity [76] and the robustness of magic [32].

Acknowledgments. — We thank M. Collura, M. Frau, A. Hamma, G. Lami, and M. Serbyn for insightful discussions. We especially thank Lorenzo Piroli for pointing out the connection between the stabilizer nullity and the SRE. P.S.T. acknowledges support from the Simons Foundation through Award 284558FY19 to the ICTP. M.D. and E.T. were partly supported by the MIUR Programme FARE (MEPH), by QUANTERA DYNAMITE PCI2022-132919, and by the EU-Flagship programme Pasquans2. M.D. was partly supported by the PNRR MUR project PE0000023-NQSTI. M.D. work was in part supported by the International Centre for Theoretical Sciences (ICTS) for participating in the program - Periodically and quasi-periodically driven complex systems (code: ICTS/pdcs2023/6). M.C.B. was partly supported by the DFG (German Research Foundation) under Germany’s Excellence Strategy – EXC-2111 – 390814868; and by the EU-QUANTERA project TNiSQ (BA 6059/1-1).

Our numerical simulations have been performed using C++ iTensor library [77].

Note added: while completing this manuscript, we became aware of a parallel, independent work on nonstabilizerness and tensor networks by Lami and Collura, introducing novel sampling methods applicable to stabilizer nullity. The work will appear on the same arxiv post.

[1] P. W. Shor, *SIAM Journal on Computing* **26**, 1484 (1997).

- [2] J. Preskill, [arXiv preprint arXiv:1203.5813](#) (2012).
- [3] L. Amico, R. Fazio, A. Osterloh, and V. Vedral, *Rev. Mod. Phys.* **80**, 517 (2008).
- [4] J. Eisert, M. Cramer, and M. B. Plenio, *Rev. Mod. Phys.* **82**, 277 (2010).
- [5] J. I. Cirac and P. Zoller, *Nature Physics* **8**, 264 (2012).
- [6] I. Bloch, J. Dalibard, and S. Nascimbène, *Nature Physics* **8**, 267 (2012).
- [7] A. Aspuru-Guzik and P. Walther, *Nature Physics* **8**, 285 (2012).
- [8] A. A. Houck, H. E. Türeci, and J. Koch, *Nature Physics* **8**, 292 (2012).
- [9] L. M. K. Vandersypen and I. L. Chuang, *Rev. Mod. Phys.* **76**, 1037 (2005).
- [10] M. B. Plenio and S. S. Virmani, in *Quantum Information and Coherence* (Springer International Publishing, 2014) pp. 173–209.
- [11] M. A. Nielsen and I. L. Chuang, *Quantum Computation and Quantum Information* (Cambridge University Press, 2012).
- [12] D. Gottesman, *Stabilizer codes and quantum error correction* (California Institute of Technology, 1997).
- [13] D. Gottesman, *Phys. Rev. A* **57**, 127 (1998).
- [14] S. Aaronson and D. Gottesman, *Phys. Rev. A* **70**, 052328 (2004).
- [15] D. Gottesman, *Phys. Rev. A* **54**, 1862 (1996).
- [16] S. Bravyi and A. Kitaev, *Phys. Rev. A* **71**, 022316 (2005).
- [17] S. Bravyi and J. Haah, *Phys. Rev. A* **86**, 052329 (2012).
- [18] E. T. Campbell, B. M. Terhal, and C. Vuillot, *Nature* **549**, 172 (2017).
- [19] A. W. Harrow and A. Montanaro, *Nature* **549**, 203 (2017).
- [20] V. Veitch, S. H. Mousavian, D. Gottesman, and J. Emerson, *New Journal of Physics* **16**, 013009 (2014).
- [21] W. K. Wootters, *Annals of Physics* **176**, 1 (1987).
- [22] D. Gross, *Journal of mathematical physics* **47** (2006).
- [23] V. Veitch, C. Ferrie, D. Gross, and J. Emerson, *New Journal of Physics* **14**, 113011 (2012).
- [24] X. Wang, M. M. Wilde, and Y. Su, *New Journal of Physics* **21**, 103002 (2019).
- [25] E. Chitambar and G. Gour, *Reviews of modern physics* **91**, 025001 (2019).
- [26] E. Wigner, *Phys. Rev.* **40**, 749 (1932).
- [27] D. Gross, *Applied Physics B* **86**, 367 (2006).
- [28] R. Hudson, *Reports on Mathematical Physics* **6**, 249 (1974).
- [29] V. Bužek, A. Vidiella-Barranco, and P. L. Knight, *Phys. Rev. A* **45**, 6570 (1992).
- [30] S. Bravyi and D. Gosset, *Phys. Rev. Lett.* **116**, 250501 (2016).
- [31] S. Bravyi, G. Smith, and J. A. Smolin, *Phys. Rev. X* **6**, 021043 (2016).
- [32] M. Howard and E. Campbell, *Phys. Rev. Lett.* **118**, 090501 (2017).
- [33] M. Heinrich and D. Gross, *Quantum* **3**, 132 (2019).
- [34] X. Wang, M. M. Wilde, and Y. Su, *Phys. Rev. Lett.* **124**, 090505 (2020).
- [35] A. Heimendahl, F. Montealegre-Mora, F. Vallentin, and D. Gross, *Quantum* **5**, 400 (2021).
- [36] T. Haug and M. Kim, *PRX Quantum* **4**, 010301 (2023).
- [37] L. Leone, S. F. E. Oliviero, and A. Hama, *Phys. Rev. Lett.* **128**, 050402 (2022).
- [38] T. Haug and L. Piroli, *Quantum* **7**, 1092 (2023).
- [39] T. Haug and L. Piroli, *Phys. Rev. B* **107**, 035148 (2023).
- [40] G. Lami and M. Collura, *Phys. Rev. Lett.* **131**, 180401 (2023).
- [41] P. S. Tarabunga, E. Tirrito, T. Chanda, and M. Dalmonte, *PRX Quantum* **4**, 040317 (2023).
- [42] P. S. Tarabunga and C. Castelnuovo, “Magic in generalized rokhsar-kivelson wavefunctions,” (2023), [arXiv:2311.08463 \[quant-ph\]](#).
- [43] E. Tirrito, P. S. Tarabunga, G. Lami, T. Chanda, L. Leone, S. F. E. Oliviero, M. Dalmonte, M. Collura, and A. Hama, “Quantifying non-stabilizerness through entanglement spectrum flatness,” (2023), [arXiv:2304.01175](#).
- [44] X. Turkeshi, M. Schirò, and P. Sierant, “Measuring magic via multifractal flatness,” (2023), [arXiv:2305.11797 \[quant-ph\]](#).
- [45] P. S. Tarabunga, “Critical behaviours of non-stabilizerness in quantum spin chains,” (2023), [arXiv:2309.00676 \[quant-ph\]](#).
- [46] C. D. White, C. Cao, and B. Swingle, *Phys. Rev. B* **103**, 075145 (2021).
- [47] F. Verstraete, V. Murg, and J. Cirac, *Adv. Phys.* **57**, 143 (2008).
- [48] U. Schollwöck, *Ann. Phys.* **326**, 96 (2011).
- [49] R. Orús, *Annals Phys.* **349**, 117 (2014).
- [50] P. Silvi, F. Tschirsich, M. Gerster, J. Jünemann, D. Jaschke, M. Rizzi, and S. Montangero, *SciPost Phys. Lect. Notes* , 8 (2019).
- [51] K. Okunishi, T. Nishino, and H. Ueda, *J. Phys. Soc. Jpn* **91**, 062001 (2022).
- [52] M. C. Bañuls, *Annu. Rev. Condens. Matter Phys* **14**, null (2023).
- [53] D. Bluvstein, S. J. Evered, A. A. Geim, S. H. Li, H. Zhou, T. Manovitz, S. Ebadi, M. Cain, M. Kalinowski, D. Hangleiter, J. P. B. Ataiades, N. Maskara, I. Cong, X. Gao, P. S. Rodriguez, T. Karolyshyn, G. Semeghini, M. J. Gullans, M. Greiner, V. Vuletić, and M. D. Lukin, *Nature* (2023), [10.1038/s41586-023-06927-3](#).
- [54] M. Beverland, E. Campbell, M. Howard, and V. Kliuchnikov, *Quantum Science and Technology* **5**, 035009 (2020).
- [55] X. Turkeshi, A. Dymarsky, and P. Sierant, “Pauli spectrum and magic of typical quantum many-body states,” (2023), [arXiv:2312.11631 \[quant-ph\]](#).
- [56] Although the probability distribution $\Xi(\alpha)$ differs from the one employed in Ref. [36], which utilizes the probability distribution of Pauli strings obtained from two-copy Bell measurements, both definitions of the Bell magic are mathematically equivalent.
- [57] D. Gross, S. Nezami, and M. Walter, *Communications in Mathematical Physics* **385**, 1325 (2021).
- [58] See supplemental material.
- [59] We note that, since $|P^{(n)}(\psi)\rangle$ is real, the computation of the norm does not require complex conjugation.
- [60] J. J. García-Ripoll, *New Journal of Physics* **8**, 305–305 (2006).
- [61] Notice that we aim to compute the same object as the method in Ref. [39], namely the expectation value of $2n$ replicas of Pauli operators. The computational advantage of our approach stems from reorganizing the order of contractions and applying a controlled approximation. Notice also that the physical dimension in our approach is constantly 4, while Ref. [39] requires a physical dimension of $2^{2(n-1)}$, which grows exponentially with n .

- [62] M. C. Bañuls, M. B. Hastings, F. Verstraete, and J. I. Cirac, *Phys. Rev. Lett.* **102**, 240603 (2009).
- [63] A. Müller-Hermes, J. I. Cirac, and M. C. Bañuls, *New Journal of Physics* **14**, 075003 (2012).
- [64] M. Hastings and R. Mahajan, *Physical Review A* **91**, 032306 (2015).
- [65] R. Orús, *Phys. Rev. B* **85**, 205117 (2012).
- [66] M. Levin and C. P. Nave, *Phys. Rev. Lett.* **99**, 120601 (2007).
- [67] Ref. [38] proves that the SRE is not a strong monotone for any finite index n . Their argument does not extend to the limit $n \rightarrow \infty$.
- [68] B.-B. Chen, L. Chen, Z. Chen, W. Li, and A. Weichselbaum, *Phys. Rev. X* **8**, 031082 (2018).
- [69] A. J. Ferris and G. Vidal, *Phys. Rev. B* **85**, 165146 (2012).
- [70] A. Montanaro, “Learning stabilizer states by bell sampling,” (2017), [arXiv:1707.04012](https://arxiv.org/abs/1707.04012) [quant-ph].
- [71] L. Leone, S. F. E. Oliviero, and A. Hamma, “Learning t-doped stabilizer states,” (2023), [arXiv:2305.15398](https://arxiv.org/abs/2305.15398) [quant-ph].
- [72] S. Grewal, V. Iyer, W. Kretschmer, and D. Liang, “Efficient learning of quantum states prepared with few non-clifford gates,” (2023), [arXiv:2305.13409](https://arxiv.org/abs/2305.13409) [quant-ph].
- [73] D. Hangleiter and M. J. Gullans, “Bell sampling from quantum circuits,” (2023), [arXiv:2306.00083](https://arxiv.org/abs/2306.00083) [quant-ph].
- [74] M. Bejan, C. McLauchlan, and B. Béri, “Dynamical magic transitions in monitored clifford+t circuits,” (2023), [arXiv:2312.00132](https://arxiv.org/abs/2312.00132) [quant-ph].
- [75] G. E. Fux, E. Tirrito, M. Dalmonte, and R. Fazio, “Entanglement-magic separation in hybrid quantum circuits,” (2023), [arXiv:2312.02039](https://arxiv.org/abs/2312.02039) [quant-ph].
- [76] S. Bravyi, D. Browne, P. Calpin, E. Campbell, D. Gosset, and M. Howard, *Quantum* **3**, 181 (2019).
- [77] M. Fishman, S. R. White, and E. M. Stoudenmire, *SciPost Phys. Codebases*, 4 (2022).
- [78] A. Gu, L. Leone, S. Ghosh, J. Eisert, S. Yelin, and Y. Quek, “A little magic means a lot,” (2023), [arXiv:2308.16228](https://arxiv.org/abs/2308.16228).
- [79] H. Hamaguchi, K. Hamada, and N. Yoshioka, “Handbook for efficiently quantifying robustness of magic,” (2023), [arXiv:2311.01362](https://arxiv.org/abs/2311.01362) [quant-ph].
- [80] I. P. McCulloch, *Journal of Statistical Mechanics: Theory and Experiment* **2007**, P10014–P10014 (2007).
- [81] U. Schollwöck, *Annals of Physics* **326**, 96–192 (2011).
- [82] E. M. Stoudenmire and S. R. White, *New Journal of Physics* **12**, 055026 (2010).
- [83] M. Frías Pérez, M. Mariën, D. Pérez García, M. C. Bañuls, and S. Iblisdir, *SciPost Physics* **14** (2023), [10.21468/scipostphys.14.5.123](https://doi.org/10.21468/scipostphys.14.5.123).

SUPPLEMENTAL MATERIAL

We present additional information on (1) the properties of the stabilizer entropy, stabilizer nullity, and Bell magic, (2) generalization to MPO, (3) generalization to qudits, (4) the MPS compression, (5) possibility for doing transverse contractions, and (6) additional numerical results.

Measures of nonstabilizerness

Stabilizer Rényi entropy

In this section, we define the stabilizer Rényi entropy and we briefly state some of its key properties to allow easy access to the main results of the paper.

Consider the $d = 2^N$ -dimensional Hilbert space of N qubits $\mathcal{H} \simeq \mathbb{C}^{\otimes 2N}$. Let us call \mathcal{P}_N the group of all N -qubit Pauli operators with phase 1, and define $\Xi_\psi(P) = d^{-1} \text{tr}(P\Psi) = \langle P \rangle_\psi$ as the squared (normalized) expectation value of P in the pure state $|\psi\rangle$ with density matrix $\Psi = |\psi\rangle\langle\psi|$. Moreover, Ξ_ψ is the probability of finding P in the representation of the state $|\psi\rangle$.

The SREs is defined in the Eq. 3. For three common choices of n the stabilizer Rényi entropy (as defined in Eq. (??) of the main text) reads

$$M_n(|\psi\rangle) = \begin{cases} \log_2(|\{P \in \mathcal{P}_N : \langle P \rangle_\psi \neq 0\}|) - N & n \rightarrow 0 \\ -\sum_P 2^{-N} \langle P \rangle_\psi^2 \log_2\left(\langle P \rangle_\psi^2\right) & n \rightarrow 1 \\ -\log_2\left(\sum_P 2^{-N} \langle P \rangle_\psi^4\right) & n = 2 \end{cases} \quad (\text{S1})$$

where $P \in \mathcal{P}_N$ is an element of the group of all N -qubit Pauli strings with +1 phases. We list some key properties of the stabilizer α -Rényi entropies, alongside the references that contain the respective proofs:

Faithfulness: $M_n(|\psi\rangle) = 0$ if and only if $|\psi\rangle$ is a stabilizer state (see Ref. [37]).

Stability under free operations: For any unitary Clifford operator C and state $|\psi\rangle$ it holds that $M_n(C|\psi\rangle) = M_n(|\psi\rangle)$ (see Ref. [37]).

Additivity: $M_n(|\psi\rangle \otimes |\phi\rangle) = M_n(|\psi\rangle) + M_n(|\phi\rangle)$ (see Ref. [37]).

Bounded: For any N -qubit state $|\psi\rangle$ it holds that $0 \leq M_n(|\psi\rangle) < N$ (see Ref. [37]).

$M_{n'}(|\psi\rangle) < M_n(|\psi\rangle)$ for $n' > n$ (see Ref. [38]).

The stabilizer entropies constitute a lower bound to the so-called T -count $t(|\psi\rangle)$ of a state: $M_n(|\psi\rangle) < t(|\psi\rangle)$ (see Ref. [78]).

For $\alpha > 1/2$ the stabilizer entropies constitute a lower bound to the so-called ‘‘robustness of magic’’: $M_n(|\psi\rangle) < \mathcal{R}_\psi$ where $\mathcal{R}_\psi = \min_x \{ \|x\|_1 \mid |\psi\rangle\langle\psi| = \sum_i x_i \sigma_i, \sigma_i \in STAB \}$ (see Refs. [33, 37]).

Bell magic

In this section, we discuss the properties of Bell magic. Its definition is

$$\mathcal{B} = \sum \Xi(\bar{r})\Xi(\bar{r}')\Xi(\bar{q})\Xi(\bar{q}') \|\sigma_{\bar{r}\oplus\bar{r}'}, \sigma_{\bar{q}\oplus\bar{q}'}\|_\infty, \quad (\text{S2})$$

where $\Xi(\bar{r})$ is the probability of the outcome \bar{r} if we perform the Bell measurement on two copies of pure state $|\psi\rangle \otimes |\psi\rangle$

$$\Xi(\bar{r}) = \langle \psi | \langle \psi | O_{\bar{r}} | \psi \rangle | \psi \rangle = 2^{-N} |\langle \psi | \sigma_{\bar{r}} | \psi^* \rangle|^2, \quad (\text{S3})$$

with $O_{\bar{r}} = |\sigma_{\bar{r}}\rangle\langle\sigma_{\bar{r}}|$ is a projector onto a product of Bell states and $|\psi^*\rangle$ denotes the complex conjugate of $|\psi\rangle$. The infinity norm is zero when the Pauli strings commute. As a measure of magic, $\mathcal{B} = 0$ only for pure stabilizer states $|\psi_{\text{STAB}}\rangle$ and $\mathcal{B} > 0$ otherwise. \mathcal{B} is also invariant under Clifford circuits U_C that map stabilizers to stabilizers for

example $\mathcal{B}(U_C|\psi\rangle)$. Moreover, Bell magic is constant under composition with any stabilizer state, i.e. if $|\psi_{\text{STAB}}\rangle$ then $\mathcal{B}(|\psi\rangle \otimes |\psi_{\text{STAB}}\rangle) = \mathcal{B}(|\psi\rangle)$. We further define the additive Bell magic:

$$\mathcal{B}_a = -\log_2(1 - \mathcal{B}). \quad (\text{S4})$$

\mathcal{B}_a has the same properties of \mathcal{B} and, further, it is also additive

$$\mathcal{B}_a(|\psi\rangle \otimes |\phi\rangle) = \mathcal{B}_a(|\psi\rangle) + \mathcal{B}_a(|\phi\rangle). \quad (\text{S5})$$

Moreover, \mathcal{B}_a has the operational meaning as the number of initial magic states $|T\rangle$. For example, if we consider the state $|\psi\rangle = |T\rangle^{\otimes k} \otimes |0\rangle^{\otimes N-k}$ consisting of a tensor product of k magic states and otherwise the stabilizer state $|0\rangle$, then the additive Bell magic is

$$\mathcal{B}_a(|T\rangle^{\otimes k} \otimes |0\rangle^{\otimes N-k}) = k. \quad (\text{S6})$$

Stabilizer nullity

In this section, we introduce the stabilizer nullity, a function $\nu(|\psi\rangle)$ of any pure state $|\psi\rangle$ that is non-increasing under stabilizer operations. The stabilizer nullity is surprisingly powerful given its simplicity: it is the number of qubits that $|\psi\rangle$ is hosted in, minus the number of independent Pauli operators that stabilize $|\psi\rangle$.

Before introducing the definition of nullity, let us first recall the definition of a stabilizer state and introduce a slight generalization of it. Let $|\psi\rangle$ be a non-zero n -qubit state. The stabilizer of $|\psi\rangle$, denoted $\text{Stab}(|\psi\rangle)$, is the sub-group of the Pauli group P_N on N qubits for which $|\psi\rangle$ is a $+1$ eigenstate, that is $\text{Stab}(|\psi\rangle) = \{P \in P_N : P|\psi\rangle = |\psi\rangle\}$. The states for which the size of the stabilizer is 2^N are called stabilizer states. States for which the stabilizer contains only the identity matrix are said to have a trivial stabilizer. If Pauli P is in $\text{Stab}(|\psi\rangle)$, we say that P stabilizes $|\psi\rangle$. Now we can define the stabilizer nullity as

$$\nu(|\psi\rangle) = N - \log(|\text{Stab}(\psi)|). \quad (\text{S7})$$

Moreover, one of the most important property of $\text{Stab}(\psi)$ is that let P be an N -qubit Pauli matrix and suppose that the probability of a $+1$ outcome when measuring P on $|\psi\rangle$ is non-zero. Then there are two alternatives for the state $|\phi\rangle$ after the measurement: either $\text{Stab}(|\phi\rangle) = \text{Stab}(|\psi\rangle)$, or $\text{Stab}(|\phi\rangle) \geq 2\text{Stab}(|\psi\rangle)$, both of which satisfy $\nu(|\phi\rangle) < \nu(|\psi\rangle)$. Following this previous property of $\text{Stab}(|\psi\rangle)$, it is easy to demonstrate that the stabilizer nullity ν is invariant under Clifford unitaries, is non-increasing under Pauli measurements, and is additive under the tensor product. Moreover, as $\nu = 0$ when $|\psi\rangle$ is a stabilizer state, the stabilizer nullity is invariant under the inclusion or removal of stabilizer states.

Generalization to matrix product operators

The technique presented in the main text can be straightforwardly adapted to matrix product operators (MPO), which represent mixed states. We consider a density matrix O of N qubits represented in the following MPO form:

$$O = \sum_{\mathbf{s}, \mathbf{s}'} U_1^{s_1, s'_1} U_2^{s_2, s'_2} \dots U_N^{s_N, s'_N} |s_1, \dots, s_N\rangle \langle s'_1, \dots, s'_N| \quad (\text{S8})$$

with $U_i^{s_i, s'_i}$ being $\chi \times \chi$ matrices, except at the left (right) boundary where U^{s_1, s'_1} (or U^{s_N, s'_N}) is a $1 \times \chi$ ($\chi \times 1$) row (column) vector.

The Pauli vector $|P(O)\rangle$ can be obtained in a similar way as in MPS, namely

$$|P(O)\rangle = \sum_{\alpha} V_1^{\alpha_1} V_2^{\alpha_2} \dots V_N^{\alpha_N} |\alpha_1, \dots, \alpha_N\rangle \quad (\text{S9})$$

where $V_i^{\alpha_i} = \sum_{a,b} \langle a | P_{\alpha_i} | b \rangle U_i^{a,b} / \sqrt{2}$ are $\chi \times \chi$ matrices. The procedure above can be seen as MPO version of the method recently discussed in Ref. [79] to obtain Pauli vector representation from the full density matrix. Notice that, unlike in the MPS case, in this case the bond dimension remains the same. Indeed, the transformation above is simply a local basis transformation from the computational basis to the Pauli basis. Note also that the norm of $|P(O)\rangle$ is $\text{Tr}[O^2]$, which is generally different from 1. Using $|P(O)\rangle$, one can compute the SRE, nullity and the Bell magic of O in the same way as in the MPS case (see Main text). However, we note that these measures of nonstabilizerness are only faithful for pure states. Nevertheless, we expect that this technique could be useful, e.g., to compute the mana [20, 23, 24], which is a good nonstabilizerness measure for mixed states.

Generalization to qudits

The generalization to d -state qudits is straightforward, by considering the d^2 generalized Pauli operators defined for qudits. With this, one can gain access to the qudit SRE for integer $n > 1$. One key difference with the qubit case is that the Pauli operators are not Hermitian for $d > 2$, and thus the Pauli vector is not necessarily real.

For odd prime d , one can also consider the set of phase-space operators, defined as

$$A_0 = \frac{1}{d^N} \sum_{\mathbf{u}} P_{\mathbf{u}}, \quad A_{\mathbf{u}} = P_{\mathbf{u}} A_0 P_{\mathbf{u}}^\dagger, \quad (\text{S10})$$

which provide an orthonormal basis for Hermitian operators in $\mathbb{C}^{d^N \otimes d^N}$. In analogy to the Pauli vector, one can compute the vector containing the discrete Wigner function

$$W_\rho(\mathbf{u}) = \frac{1}{d^N} \text{Tr}(A_{\mathbf{u}} \rho). \quad (\text{S11})$$

One can then compute the mana entropy [45] for integer $n > 1$ with similar technique as the SRE. The mana itself, which corresponds to $n = 1/2$, is not accessible with the replica method. Nevertheless, one can perform sampling on the MPS containing the discrete Wigner function to compute the mana.

MPS compression

As mentioned in the main text, the MPS $|P^{(n)}(\psi)\rangle$ should be compressed to keep the cost manageable. There are a few methods to perform the compression, such as the density matrix algorithm [80], the SVD compression, and variational compression [81]. We refer to Refs. [80, 81] for details on the compression methods.

To compress the Pauli vector $|P(\psi)\rangle$, we perform the SVD compression by iteratively truncating the bond dimension to χ_P from left to right, while moving the orthonormality center. We recall that $|P(\psi)\rangle$ without compression is automatically orthonormalized, which implies that the compression is (globally) optimal. The overall cost of the compression is $O(\chi_P^2 \chi^2 + \chi^3 \chi_P)$.

Similar SVD compression can be performed to compress the MPO-MPS multiplication $W|P(\psi)\rangle$. However, the resulting MPS is no longer orthonormalized, and the considerations above do not apply. Nevertheless, as argued in Refs. [81, 82], the SVD compression in the MPO-MPS product would still yield a good result, particularly if both the MPO and MPS are orthonormalized (which is true in our case).

In our computations of the SRE and the Bell magic, we have performed the compression using only the SVD compression. We have checked with bond dimension up to $\chi_P = 100$ that the results using the SVD compression is consistent with the solution obtained by the density matrix algorithm, which is optimal but more costly.

To calculate the stabilizer nullity, we find that the density matrix algorithm is more reliable to obtain the correct result. Therefore, we used the density matrix algorithm to obtain the stabilizer nullity of the Ising and XXZ chain. However, the density matrix algorithm is too costly for the simulation of random Clifford circuits. In that case, we instead perform SVD compression followed by variational compression.

Transverse contraction

An alternative way to perform the contraction of the two-dimensional tensor network in Fig. 1 (c) is by contracting the tensors in the transversal (space) direction [62–64]. To do so, we first contract the $2n$ tensors in the first site to form a transfer matrix with $2n$ indices, each with bond dimension χ^2 . Then, we iteratively absorb the tensors on the right to the transfer matrix, up until the rightmost tensors. Without compression, the cost of this contraction scheme is $O(\chi^{4n+2})$, which is cheaper than the exact contraction in the direction of Rényi index, or the contraction in Ref. [39]. Of course, the contractions can also be done approximately by representing the transfer matrix as an MPS. Whether or not this would yield a better performance compared to the approximate contraction in the direction of Rényi index is an intriguing question that we leave for future research avenue.

In the case of translation-invariant (TI) MPS in the thermodynamic limit, we can compute the SRE by introducing

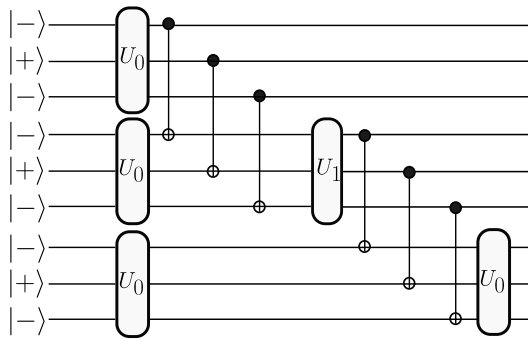


FIG. S1. The scrambling circuit recently experimentally realized in Ref. [53] to measure the additive Bell magic for $N = 9$. The gates U_0 and U_1 are as defined in Ref. [53].

the transfer matrix

$$\begin{aligned} \tau &= \sum_{\alpha} B^{(n)\alpha} \otimes B^{(n)\alpha} \\ &= \sum_{\alpha} (B^{\alpha})^{\otimes 2n}. \end{aligned} \quad (\text{S12})$$

Here, we recall that $B^{(n)\alpha}$ is the local tensor of $|P^{(n)}(\psi)\rangle$, which is site independent for TI MPS. The transfer matrix τ is identical to the one introduced in Ref. [39], however the local tensors that build τ differ. In particular, with our approach, the transfer matrix can be viewed as an MPO with physical dimension χ^2 and constant bond dimension of 4, i.e., the MPO satisfies an area law. The calculation of the SRE is then reduced to the computation of the dominant eigenvalue of τ . This can be done by approximating the dominant eigenvector $|L\rangle$ as an MPS, and performing power iteration or Lanczos algorithm by repeated MPO-MPS multiplication.

Additional numerical results

Convergence with bond dimension in replica MPS

In our simulations, we have studied the accuracy of our approach by checking the convergence of our results with bond dimension. Fig. S2 illustrates an example of the dependence of the SRE m_2 in the ground state of the XXZ chain. In particular, we studied the effect of increasing χ , χ_P and χ_2 . We see that as the bond dimensions are increased, the SRE eventually converges to a constant. Interestingly, we find that χ_2 can be set to a smaller value than χ_P . In Fig. S2 (d), we show that the decay of the error as a function of the bond dimension appears to be exponential, consistent with the findings of Ref. [39].

Bell magic

We perform benchmarking simulations of the additive Bell magic in the ground states of the Ising and XXZ chains, shown in Fig. S3 (a) and (b), respectively. We find that the additive Bell magic exhibits similar behavior to that of the SRE [38, 39]. Moreover, we investigated the growth of the Bell magic under random Clifford circuits doped with a single T gate per time step. Here the circuit is a brickwork of two-site Clifford gates chosen randomly from the set $\{I, CNOT^L, CNOT^R\}$. The initial state is polarized in the y direction, and the T gates are applied to a randomly chosen site at each time step. The results are shown in Fig. S4 (a). We observe that, at short times, the additive Bell magic grows linearly as $\mathcal{B}_a = t$.

Furthermore, we computed the Bell magic in a state prepared by a quantum circuit recently realized in Ref. [53], for $N = 9$. The relative circuit is shown in Fig. S1. Also in this case, we verify that the additive Bell magic increases as a function of the number of CCZ gates applied.

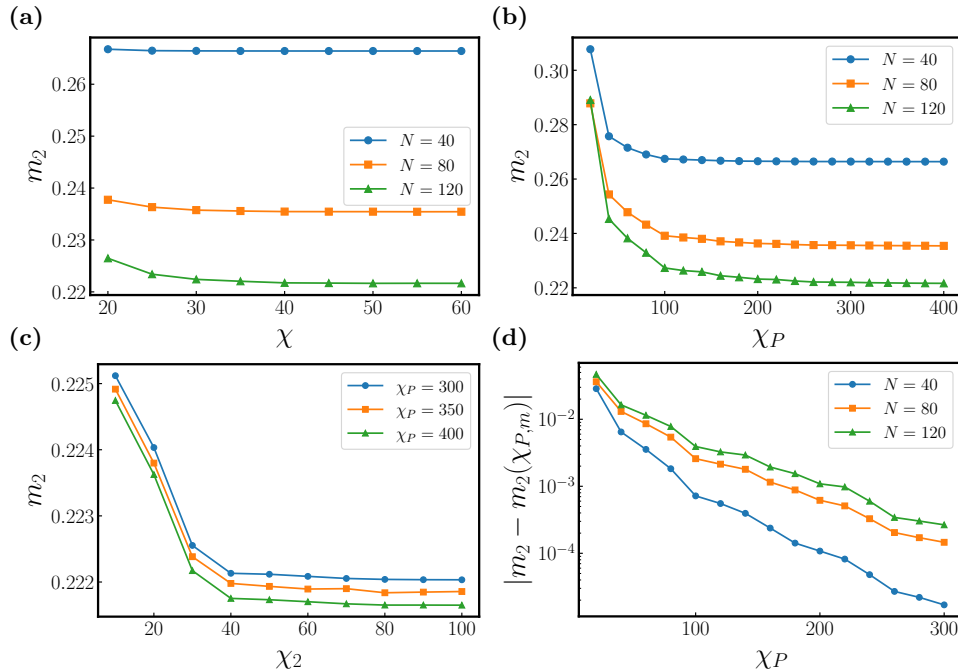


FIG. S2. SRE density $m_2 = M_2/N$ for the ground state of the XXZ chain with anisotropy $\Delta = 0.9$ (a) as a function of bond dimension χ with fixed $\chi_P = 400$ and $\chi_P^{(2)} = 100$, (b) as a function of bond dimension χ_P with fixed $\chi = 60$ and $\chi_P^{(2)} = 100$, and (c) as a function of $\chi_P^{(2)}$ with fixed $\chi_P \in \{200, 250, 300\}$ and $\chi = 60$. (d) Difference of m_2 computed for bond dimension χ_P and the maximum bond dimension $\chi_{P,m} = 400$ at fixed $\chi_P^{(2)} = 100$.

Stabilizer nullity

We present an additional result of random Clifford circuits for constant-depth circuit with $D = 10$ in Fig. S4 (b). Also in this case $-\log_2 \|\langle P_k \rangle\|$ reaches its expected value in all cases.

Perfect sampling

Here, we show that our approach can also be applied to improve methods based on tensor network sampling, which recently have been proposed to estimate the SRE [38, 40, 41]. In particular, the Pauli strings can be sampled directly according to the probability distribution $\Xi(\alpha) = |\langle \psi | P_\alpha | \psi \rangle|^2 / 2^N$ via perfect Pauli sampling algorithm introduced in [38, 40]. With the MPS representation in Pauli basis in Eq. (2), this is equivalent to the perfect MPS sampling proposed in Ref. [69] (see also Refs. [82, 83]). The cost scales as $O((\chi^2)^2) = O(\chi^4)$ with respect to the bond dimension χ_P . At first glance, this appears to be worse than the cost of perfect Pauli sampling in the MPS form of $|\psi\rangle$, which costs $O(\chi^3)$. However, similarly as in the replica method, we can truncate χ_P to a value considerably smaller than χ^2 , such that the perfect MPS sampling on Eq. (2) becomes superior to perfect Pauli sampling. The comparison between perfect sampling in $|P(\psi)\rangle$ and perfect Pauli sampling in $|\psi\rangle$ is shown in Fig. S4 (c). With our method, we find that M_1 can be converged with considerably less resources compared to the standard approach, even when accounting for the initial overhead of constructing the MPS in the Pauli basis.

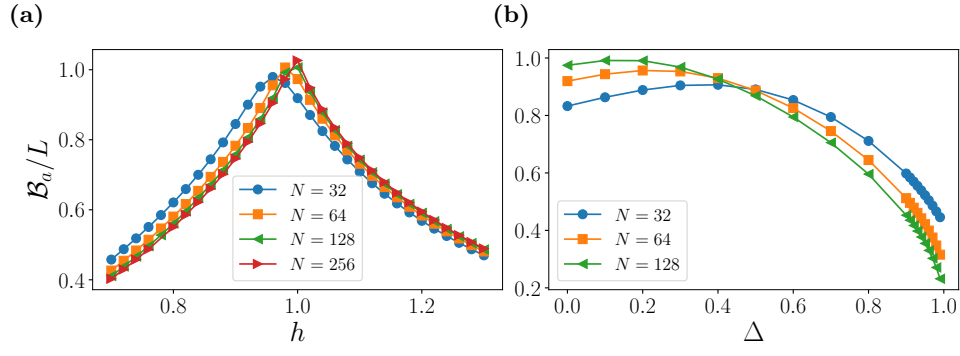


FIG. S3. The additive Bell magic density \mathcal{B}_a/N for the ground state of (a) the quantum Ising chain as a function of the transverse field h and (b) the XXZ chain as a function of the anisotropy Δ .

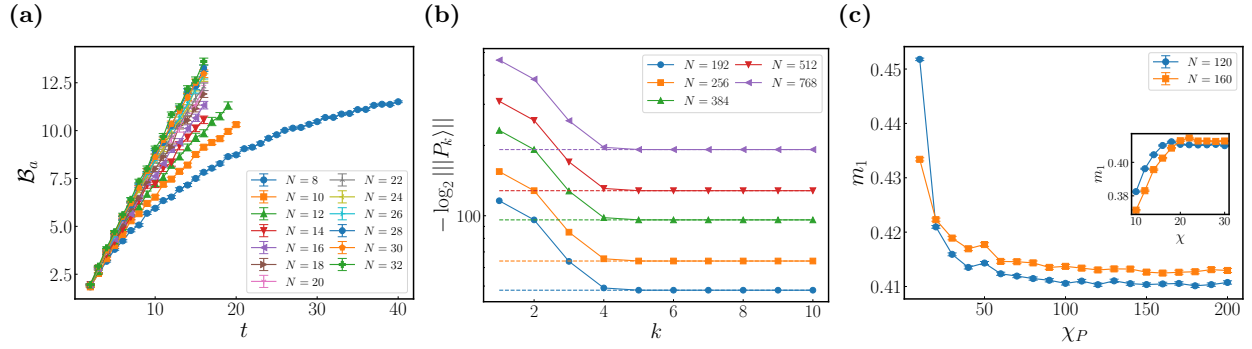


FIG. S4. (a) The additive Bell magic \mathcal{B}_a in random Clifford circuits doped with a single T gate per time step, averaged over at least 100 realizations. (b) $-\log_2 \| |P_k\rangle \|$ at iteration k in random quantum circuits with depth $D = 10$ and $N_T = N/2$ number of T gates. The dashed line denotes the analytically known $(N - \nu)/2$ for each system with the same color. (c) SRE density $m_1 = M_1/N$ calculated with perfect sampling on $|P(\psi)\rangle$. The ground state is obtained with $\chi = 60$. Inset: m_1 calculated by the perfect sampling introduced in Ref. [38, 40]. Both results are for the ground state of the XXZ chain with anisotropy $\Delta = 0.9$ and system size $N \in \{120, 160\}$. The number of sample is $N_S = 10^5$.